IL NUOVO CIMENTO Vol. 34 C, N. 3 Maggio-Giugno 2011
DOI 10.1393/ncc/i2011-10895-8

Colloquia: Scineghe2010

Constraining decaying dark matter with FERMI-LAT gamma rays

L. Maccione
DESY, Theory Group - Notkestraße 85, D-22607 Hamburg, Germany

(ricevuto il 25 Febbraio 2011; pubblicato online l'1 Giugno 2011)

Summary. — High energy electrons and positrons from decaying dark matter can produce a significant flux of gamma rays by inverse Compton off low energy photons in the interstellar radiation field. This possibility is inevitably related with the dark matter interpretation of the observed PAMELA and FERMI excesses. We will describe a simple and universal method to constrain dark matter models which produce electrons and positrons in their decay by using the FERMI-LAT gamma-ray observations in the energy range between 0.5 GeV and 300 GeV, by exploiting universal response functions that, once convolved with a specific dark matter model, produce the desired constraint. The response functions contain all the astrophysical inputs. We discuss the uncertainties in the determination of the response functions and apply them to place constraints on some specific dark matter decay models that can well fit the positron and electron fluxes observed by PAMELA and FERMI LAT, also taking into account prompt radiation from the dark matter decay. With the available data decaying dark matter cannot be excluded as source of the PAMELA positron excess.

PACS 95.35.+d – Dark matter (stellar, interstellar, galactic, and cosmological).
PACS 98.70.Vc – Background radiations.

1. – Introduction

The existence of dark matter (DM) in our Universe is nowadays a widely accepted fact. DM constitutes the dominant fraction of matter present in the Universe. However, all the astrophysical evidences for DM, such as those coming from gravitational lensing, galaxy rotation curves and cosmic microwave background (CMB) anisotropies, are purely gravitational [1], and its particle nature remains unknown.

The most popular type of DM candidate, a weakly interacting massive particle (WIMP), can naturally reproduce the observed DM abundance due to effective self-annihilation in the early Universe. Today, this same annihilation process could produce an observable contribution to the measured cosmic-ray fluxes on Earth [2] and have impact on cosmological observations [3]. However, such an indirect detection of DM is also possible if DM *decays* at a sufficiently large rate. Indeed, there exists a number of interesting and theoretically well motivated DM models that *predict* the decay of DM

on cosmological time scales, with lifetimes around and above $\tau_\chi \simeq \mathcal{O}(10^{26}\,\mathrm{s})$. Among the candidate models we have the gravitino in small R-parity breaking scenarios, sterile neutrinos, kinetically mixed hidden gauge bosons and gauginos (see refs. in [4]).

On the observational side, recent results by several Cosmic Ray (CR) and γ-ray experiments have seriously challenged the standard description and interpretation of the generation of high-energy CR electrons, positrons and γ-rays, thus giving room also to DM interpretations. In particular, the PAMELA satellite reported the presence of an increase in the positron fraction $J(e^+)/J(e^+ + e^-)$ above 10 GeV [5], which was not expected in theoretical models, while the $e^- + e^+$ spectra from FERMI LAT [6] and H.E.S.S. [7] revealed features hardly compatible with current theoretical models.

High energy CR electrons and positrons produce γ-rays through the processes of inverse Compton scattering (ICS) off low energy photons in the interstellar radiation field (ISRF) and through bremsstrahlung emission due to the interaction with the interstellar medium (ISM). The FERMI Gamma-Ray Space Telescope is currently observing the γ-ray sky in the energy range between 30 MeV and 300 GeV with unprecedented angular resolution and precise energy sensitivity.

It proves useful to develop model-independent analysis tools such as response functions. These are functions of injected electron or positron energy which are obtained from comparing the γ-ray spectrum resulting on Earth after propagation (which we call signal) with the observed γ-ray spectrum (which henceforth will be called background). While they encode information about propagation of $e^\pm$ in the Galaxy, response functions are independent of the particle physics model leading to the actual $e^\pm$ spectra. Hence, constraints can be obtained by the convolution of the $e^\pm$-response functions with a given DM decay spectrum (possibly accounting also for the prompt radiation emitted in the decay process) and requiring that the result be smaller than the product of DM mass and lifetime in suitable units. If this condition is violated, the DM model predicts γ-ray fluxes (from ICS and bremsstrahlung) that are higher than the data by at least 2σ.

2. – $e^\pm$-response functions from Inverse Compton Scattering

In this section we derive the $e^\pm$-response functions for the γ-ray emission induced by DM decays into electrons and positrons by comparing our predictions with the 1-year observations of FERMI LAT in the energy range of 0.5 GeV to 300 GeV.

As data we use the FERMI-LAT γ-ray maps as derived in ref. [8]. In this analysis the events were binned into the eight energy ranges 0.5–1 GeV, 1–2 GeV, 2–5 GeV, 5–10 GeV, 10–20 GeV, 20–50 GeV, 50–100 GeV and 100–300 GeV.

2˙1. *Definitions and optimal sky patch.* – Response functions are functions of the electron injection energy and are associated to γ-ray observations in a sky patch $\Delta\Omega$ and in an energy band $E_0 \le E_\gamma \le E_1$. The $e^\pm$-response functions are defined as the ratio of the predicted γ-ray fluxes resulting from decaying DM to the observed fluxes as

$$F_\gamma^{E_0:E_1}(\Delta\Omega; E_e) \equiv \frac{\int_{E_0}^{E_1} \mathrm{d}E_\gamma \int_{\Delta\Omega} \mathrm{d}\Omega J_{\mathrm{ICS}}(\Omega, E_\gamma; E_e)}{J_{\mathrm{obs}}^{E_0:E_1}(\Delta\Omega) + 2 \cdot \delta J_{\mathrm{obs}}} \left(\frac{\tau_\chi}{10^{26}\,\mathrm{s}}\right) \left(\frac{m_\chi}{100\,\mathrm{GeV}}\right), \tag{1}$$

where we adopt the conservative attitude of adding, in each energy and angular bin, to the central value of the observed flux the associated 2σ error and $J_{\mathrm{ICS}}(\Omega, E_\gamma; E_e)$ is calculated as in [4]. Response functions depend on neither the DM lifetime τ_χ nor its

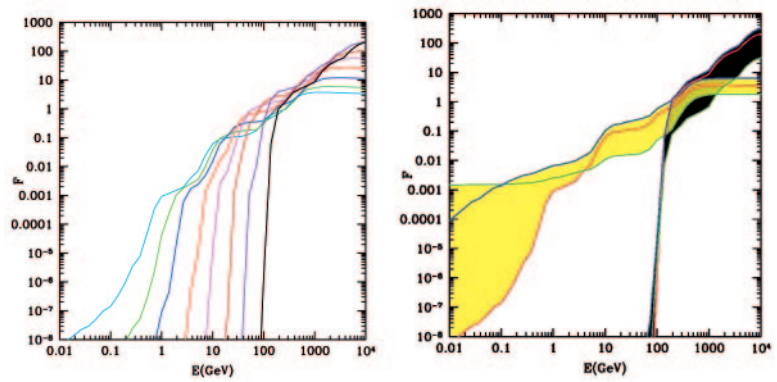

Fig. 1. – (Colour on-line) The $e^{\pm}$-response function F_γ based on γ-ray emission for the L1 model of table I. The $e^{\pm}$-response functions are derived from the eight γ-ray energy ranges 0.5–1 GeV, 1–2 GeV, 2–5 GeV, 5–10 GeV, 10–20 GeV, 20–50 GeV, 50–100 GeV, and 100–300 GeV from top to bottom at left side, respectively. The underlying sky patch $\mathcal{S}$ is defined by $|l| \leq 20^\circ$ and $-18^\circ \leq b \leq -10^\circ$. The propagation model dependence of the $e^{\pm}$-response function F_γ based on our fixed patch for the γ-ray energy range 0.5–1 GeV (yellow band, curves extending to low energies) and 100–300 GeV (black band, curves cutting off around 100 GeV). The width of the bands represents the variation within the MIN (green, top on left side), L1 (red, bottom of left side) and MAX (blue, middle on left side) propagation models of table I.

mass m_χ, and constraints on a given DM decay model can then be easily cast in the form

$$\int_{m_e}^{m_\chi} \mathrm{d}E_e \, F_\gamma^{E_0:E_1}(\Delta\Omega; E_e) \frac{\mathrm{d}N_e}{\mathrm{d}E_e}(E_e) \leq \left(\frac{\tau_\chi}{10^{26}\,\mathrm{s}}\right)\left(\frac{m_\chi}{100\,\mathrm{GeV}}\right), \tag{2}$$

where $\mathrm{d}N_e/\mathrm{d}E_e$ is the electron/positron spectrum obtained from DM decay in some specific particle physics model. We stress again that the advantage of the $e^{\pm}$-response function approach is that the $e^{\pm}$-response functions are independent of the specific DM decay spectrum. The method is hence directly applicable to any DM model, and, moreover, allows a discussion of the typical characteristics of ICS radiation from DM decay in a model-independent way.

The $e^{\pm}$-response functions depend crucially on the chosen patch $\Delta\Omega$, which should cover the area with the largest signal-to-background ratio, maximizing the $e^{\pm}$-response functions. For the derivation of the $e^{\pm}$-response functions we will focus on the patch $\mathcal{S}$ close to the galactic center and defined by $|l| < 20^\circ$ and $-18^\circ < b < -10^\circ$ [4].

2˙2. *Response functions without foreground subtraction.* – Our results for the $e^{\pm}$-response function are shown in fig. 1 as a function of the electron/positron injection energy, for the 8 different energy ranges of FERMI-LAT skymaps from ref. [8]. The highest energy range provides the strongest constraint on decaying DM with very hard electron/positron energy spectrum. However, for lower injection energies in the 100 GeV–1 TeV region, several energy ranges give actually roughly the same constraints.

To illustrate the large uncertainties related to inverse Compton radiation from DM decay inside the diffusive halo, we show in fig. 1 (right panel) the $e^{\pm}$-response functions based on the highest and lowest γ-ray energy ranges for our three reference propagation models from table I. The uncertainties on the $e^{\pm}$-response functions are dominated by

TABLE I. – *Typical combinations of propagation parameters (see* [12, 4] *for definitions and for references to the propagation equation) that are consistent with an analysis of CR nuclei secondary/primary ratios. The MIN and MAX propagation models correspond to minimal and maximal primary antiproton fluxes, respectively* [9-11]*, while the L1 model can provide a good description of B/C,* $\bar{p}/p$ *and data on other secondary/primary ratios above* 1 GeV/n [12].

Model	δ^1	D_0 (10^{28}cm^2/s)	R (kpc)	L (kpc)	V_c (km/s)	dV_c/dz km/s/kpc	V_a (km/s)	$h_{\rm reac}$ (kpc)
MIN	0.85/0.85	0.048	20	1	13.5	0	22.4	0.1
L1	0.50/0.50	4.6	20	4	0	0	10	4
MAX	0.46/0.46	2.31	20	15	5	0	117.6	0.1

the propagation model, especially for the lower energies, below 10 GeV injection energy, where also effects of reacceleration become relevant. For higher injection energies above 10–100 GeV, where the response functions become of $\mathcal{O}(1)$ and are hence relevant for the actual bounds, the uncertainties mainly stem from the height of the diffusion zone. In effect, high energy electrons and positrons lose energy in a very short time compared to the diffusion time, thus making the other details of the propagation irrelevant. The MAX propagation model gives the strongest constraints due to its large diffusive halo, whereas the MIN propagation model minimizes the constraints. Moreover, for the MAX model re-acceleration shifts lower energy electrons to higher energies. This effect is however only relevant for electrons below around 10 GeV, and thus increases the γ-ray emission only in the MeV regime. Note that for the highest observed γ-ray energy region (100–300 GeV), one clearly finds a sharp cut off at low injection energies since γ-rays at such high energies cannot be produced from ICS of electrons/positrons injected at energies lower than 100 GeV.

It is remarkable that subtraction of standard astrophysical contributions to the γ-ray flux, such as the contribution of γ-rays due to the decay of π^0's produced in pp interactions might improve the constraining capability of the response functions by almost one order of magnitude at low energy, and by $\sim 15\%$ in the energy range 100–300 GeV [4].

3. – Constraint on dark matter models

Within a given DM model γ-rays can be produced not only as secondaries of electron and positron propagation in the Galaxy, but also as final-state, or prompt, radiation arising in the decay. For selected decay channels, we calculated the corresponding galactic and extragalactic prompt fluxes in our selected patch as described above and added them to the one described by the $e^{\pm}$-response functions in order to derive constraints that come from the total prompt + ICS radiation flux of different DM decaying models. In fig. 2 we show our results for bounds on the four different decay channels into $\mu^+\mu^-\mu^+\mu^-$, $\mu^+\mu^-$, $\tau^+\tau^-$ and $b\bar{b}$ as examples with different amount of prompt and ICS radiation. The first three decay modes can well fit the PAMELA/FERMI positron and electron data if the positron excess is interpreted in terms of decaying DM, and the preferred mass and lifetime regions are indicated by the blue blobs with red crosses inside. In these plots the dash-dotted (dotted) line shows the bounds obtained from ICS (prompt) radiation in our patch $\mathcal{S}$ alone, the thick solid line shows the bounds obtained when prompt and ICS radiation are combined. Furthermore, the bounds can be strengthened to the yellow region when the foreground model L1 is subtracted from the data.

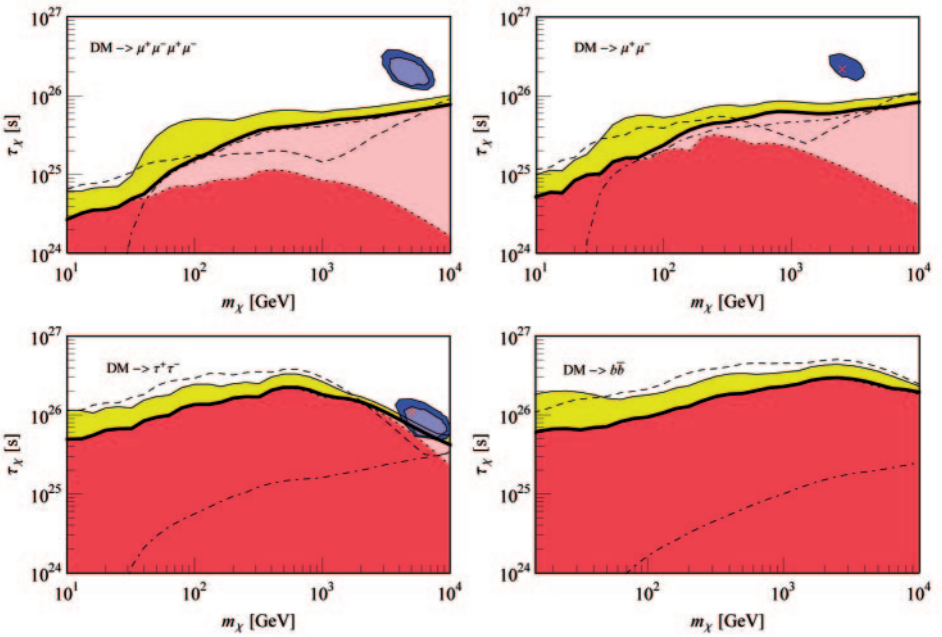

Fig. 2. – Bounds on different decay channels in the mass *vs.* lifetime plane. Regions below the thick solid line are excluded by combined ICS and prompt radiation in the L1 propagation model, whereas parameter space below the dash-dotted (dashed) line is excluded due to ICS (prompt) radiation alone. The ICS constraints shown with the dash-dotted lines are calculated from the response functions shown in fig. 1. The constraints can be strengthened to the yellow light shaded region (limited by the solid thin line) if the prediction of Model L1 for the galactic diffuse astrophysical foreground is subtracted. The blue blobs with red crosses (which are taken from ref. [13]) show the parameters that well fit electron + positron fluxes observed by FERMI LAT and H.E.S.S. and the positron fraction observed by PAMELA as described in the text.

It turns out that for decays into $\mu^+\mu^-$ pairs and four-body decay into $\mu^+\mu^-\mu^+\mu-$, the strongest constraints typically come from ICS rather than from the prompt radiation and the constraints could be improved by more than a factor of 2 for small masses and by a few 10% for large masses after removal of the γ-ray emission from conventional astrophysical sources. In the case of decay into $\tau^+\tau^-$ and $b\bar{b}$ the prompt radiation alone already provides strong constraints, which can again be improved by subtracting galactic foreground as for the case of decay into muons.

4. – Conclusions

We showed how to compute and use response functions to account for the contribution of decaying DM to the flux of high energy γ-rays, and to place constraints on the properties of decaying DM. Under the conservative assumption of a propagation model with the height of the diffusion zone around 4 kpc, based on the FERMI-LAT data, we can severely constrain but not exclude models with DM decay into $\tau^+\tau^-$ that can explain the positron excess observed by PAMELA. Moreover, we find that analogous models with two- and four-body decay channels into $\mu^\pm$s remain essentially unconstrained by current

observations. When our reference foreground model is subtracted the lower bounds on the lifetime in general increase by $\mathcal{O}(1)$ factors for DM masses below 1 TeV, and by 10–60% for masses above 1 TeV, which is however not enough to exclude the above channels in the parameter regime relevant for PAMELA. The bounds might improve by $\mathcal{O}(1)$ factors when data with better background rejection is used. For comparison we also calculated conservative bounds from the isotropic extragalactic γ-ray background as inferred from the FERMI-LAT data, finding again that even the decay into $\tau^+\tau^-$ cannot be excluded in this way.

REFERENCES

[1] Bertone G., Hooper D. and Silk J., *Phys. Rep.*, **405** (2005) 279.
[2] Ullio P., Bergstrom L., Edsjo J. and Lacey C. G., *Phys. Rev. D*, **66** (2002) 123502.
[3] Zhang L., Chen X. L., Lei Y. A. and Si Z. G., *Phys. Rev. D*, **74** (2006) 103519.
[4] Zhang L., Weniger C., Maccione L., Redondo J. and Sigl G., *J. Cosmol. Astropart. Phys.*, **1006** (2010) 027.
[5] Adriani O. *et al.* (PAMELA Collaboration), *Nature*, **458** (2009) 607.
[6] Abdo A. A. *et al.* (The Fermi LAT Collaboration), *Phys. Rev. Lett.*, **102** (2009) 181101.
[7] Aharonian F. *et al.* (H.E.S.S. Collaboration), *Phys. Rev. Lett.*, **101** (2008) 261104.
[8] Dobler G., Finkbeiner D. P., Cholis I., Slatyer T. R. and Weiner N., *Astrophys. J.*, **717** (2010) 825.
[9] Donato F., Maurin D., Salati P., Barrau A., Boudoul G. and Taillet R., *Astrophys. J.*, **563** (2001) 172.
[10] Donato F., Fornengo N., Maurin D. and Salati P., *Phys. Rev. D*, **69** (2004) 063501.
[11] Maurin D., Taillet R. and Donato F., *Astron. Astrophys.*, **394** (2002) 1039.
[12] Di Bernardo G., Evoli C., Gaggero D., Grasso D. and Maccione L., *Astropart. Phys.*, **34** (2010) 274.
[13] Ibarra A., Tran D. and Weniger C., *J. Cosmol. Astropart. Phys.*, **1001** (2010) 009.